

Numerical estimation of lagged coherency function at a hard rock site in Korea

Dongyeon Lee, Duhee Park

Department of Civil and Environmental Engineering, Hanyang University, Seoul, South Korea, dpark@hanyang.ac.kr

Jeong-Seon Park, Hak-Sung Kim, Yonghee Lee

Central Research Institute, Korea Hydro & Nuclear Power Co., Ltd., Daejeon, South Korea

ABSTRACT: Because soil is inherently non-uniform, performing incoherency Soil-Structure Interaction (SSI) analyses that account for spatial variability of ground motion can yield more realistic structural responses than the modeling the ground as laterally homogeneous. Such variability is typically represented by empirical coherency functions estimated from records obtained by dense seismic arrays. However, the installation and long-term operation of such arrays are costly. This study utilized in-situ geophysical test results from a hard rock site in Korea, to derive spatial variability parameters for the target site. These parameters were used to perform numerical modeling and develop a site-specific coherency function. The numerically derived function was then compared and validated against an empirically developed coherency function for the same site. The results showed a high degree of agreement between the numerical and empirical functions, indicating that when precise site-specific spatial variability parameters are available, numerical simulations can potentially replace empirical coherency functions. However, this study addressed only horizontal lagged coherency, and further validation for vertical lagged coherency and bidirectional plane-wave coherency functions will be required in future research.

KEYWORDS: Lagged coherency, spatial variability, numerical simulation.

1 INTRODUCTION

Soil and rock sites are inherently heterogeneous, and seismic waves generated by earthquakes do not propagate uniformly. As a result, differences in ground motion can occur even between observation points that are located close to each other (Luco & Wong, 1986; Rathje et al., 2010; Ancheta et al., 2011). Such differences can be described by ground-motion coherency, and the mathematical expression that quantifies similarity is referred to as the ground-motion coherency function. Because this function represents the relationship between ground motion similarity, station separation distance, and frequency, it inherently reflects the site-specific characteristics of the target site (Haber et al., 2021). In general, coherency decreases with increasing frequency and separation distance, and its sensitivity to individual seismic events has been reported to be relatively low (Abrahamson, 2007). Coherency function is typically developed empirically by installing dense arrays of velocimeters at target site and using the recorded ground motions. However, installing and operating such arrays over extended periods involves significant cost, making site-specific coherency estimation challenging.

Physics-based numerical simulations therefore offer a cost-effective alternative approach. Jang et al. (2017) and Lee et al. (2025) demonstrated the potential for developing site-specific functions by applying numerical simulations to the Pinyon Flat array in the western United States (Abrahamson, 2007) and validating the results against pre-established empirical functions. Nevertheless, because those studies relied on assumed spatial variability parameters in their numerical modeling, the resulting functions could not be fully validated.

This study estimates spatial variability parameters from in situ tests conducted at a rock site in Korea and utilizes them to model the target site for numerical simulations. The objective is to assess whether a site-specific coherency function for the rock site can be developed numerically by comparing the simulation results with an empirically developed coherency function (Lee et al., 2024).

2 SITE CHARACTERIZATION

This section outlines the site characterization process. The layout of the target site is shown in Figure 1, where five SPS

tests, labeled BH-1 through BH-5, were conducted to depths of up to 50 m. In addition, 16 portable seismometers (St.01–St.16) were deployed to record ambient vibrations and compute the horizontal-to-vertical spectral ratio (HVSr), from which shear-wave velocity (V_s) profiles were obtained. For the inversion process, it was necessary to define initial profiles; thus, a total of 16 were estimated based on the V_s profiles measured from the SPS tests. From the 16 portable seismometers, 16 inversions were performed, producing 256 V_s profiles in total. These profiles, along with a representative V_s profile generated by averaging and layering all cases, are presented in Figure 2.

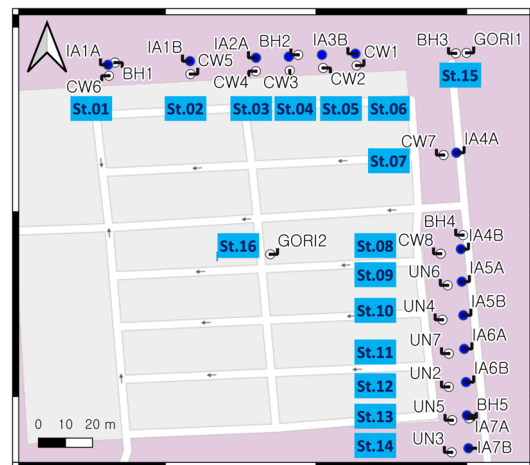


Figure 1. Locations of seismometers in dense array.

The spatial variability of the target site can be described statistically using its mean value, coefficient of variation (CV), and correlation length (CL) (Baecher et al., 2003). The CV is a statistical indicator that represents the degree of data dispersion relative to the mean. CV is expressed as follows:

$$CV = \frac{\sigma_{V_s}}{\mu_{V_s}} \quad (1)$$

where σ_{V_s} denotes the standard deviation and μ_{V_s} represents the mean V_s value within a given layer. In this study, representative V_s was taken as μ_{V_s} , after which σ_{V_s} for each layer was calculated using the measured V_s profiles (Figure 2).

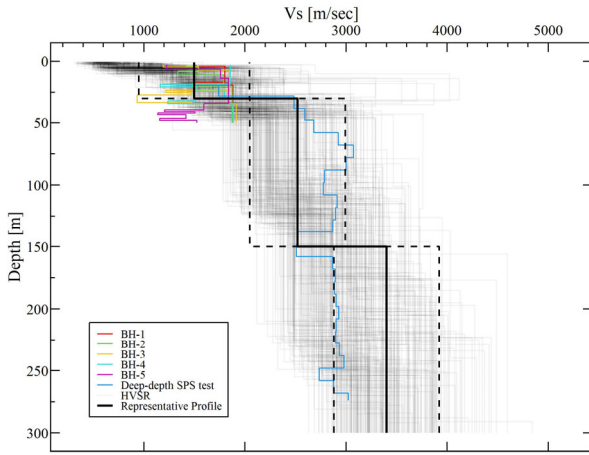


Figure 2. V_s profiles at target site.

CL is defined as the shortest distance over which ground parameter values remain correlated. It is influenced by both horizontal and vertical orientations, and distinguishing between these two directions helps capture the correlation of V_s between points in different spatial directions. Horizontal and vertical CL values were estimated separately using the corresponding separation distances. CL was derived from the spatial autocorrelation coefficient (ρ), which quantifies the relationship between two points separated by a given distance (τ). The coefficient ρ was computed using the following equation:

$$\rho(\tau) = \frac{\sum_{h=0}^{\tau_{\max}-\tau-1} (V_{S,h} - \bar{V}_S)(V_{S,h+\tau} - \bar{V}_S)}{\sum_{h=0}^{\tau_{\max}-1} (V_{S,h} - \bar{V}_S)^2} \quad (2)$$

where \bar{V}_S refers to the mean V_s , while $V_{S,h}$ and $V_{S,h+\tau}$ represent V_s values measured at two locations separated by a distance τ . As the separation distance increases, ρ gradually approaches zero. This relationship can be modeled using different regression functions. In this study, the Gaussian model was selected to compute ρ , as expressed below:

$$\rho(\tau) = \exp\left(-\pi\left(\frac{|\tau|}{CL}\right)^2\right) \quad (3)$$

where CL is taken as the value of τ at which ρ decreases by $1/e^\pi$.

For each inversion, 16 V_s profiles corresponding to the 16 measurement locations were obtained, and the CV was computed from these profiles using Equation (1). Repeating this procedure for all inversion cases yielded 16 CV values in total. This approach reflects the three-dimensional variability of the site's geological stratigraphy. The depth-dependent changes in CV are illustrated in Figure 3. The results show a rapid decrease in CV with increasing depth, indicating that variability becomes minimal beyond about 100 m and eventually stabilizes. In contrast, the highest variability occurs near the surface, particularly within the upper 30 m. Using the CV values calculated for each layer, a smoothed mean curve was generated to best fit the observed CV distribution.

To determine the CL, the dataset with closely spaced depth intervals of V_s is required. However, the V_s profiles obtained from HVSr inversion provide only a single V_s value per layer, which leads to unrealistically large CL estimates. This makes it difficult to accurately evaluate CL from HVSr-derived profiles. As an alternative, nearby SPS logging data were used, as they offer V_s measurements every 3–4 m to a depth of 100 m. In this study, these SPS results were utilized to estimate both vertical and horizontal correlation lengths (CLv and CLh). The computation of CLv and CLh involves determining the ρ for a given separation distance. For CLv, ρ was calculated using the

vertical distribution of V_s residuals, and CLv was obtained as a fitted parameter. For CLh, ρ was calculated from V_s residuals between profiles separated horizontally, with CLh similarly determined as a fitted parameter. Equation (3) was applied as the fitting function for the ρ . The spatial variability parameters derived for the target site are summarized in Table 1.

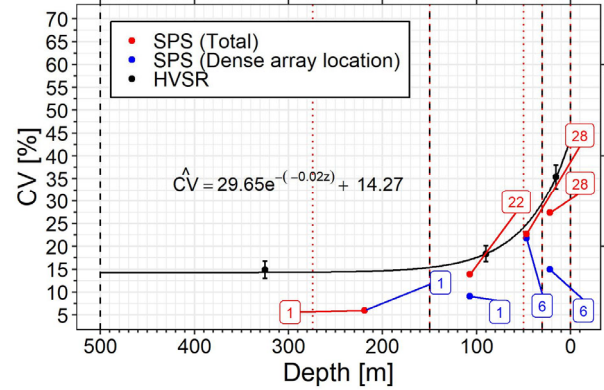


Figure 3. CVs at each layer.

Table 1. V_s and spatial variability parameters of target site.

Layer	Depth (m)	V_s (m/sec)	CV (%)	CLv (m)	CLh (m)
1	0-30	1,546	35	9.8	23.3
2	30-150	2,302	19	13	32.1
3	150-500	3,487	13	-	-

3 EMPIRICAL LAGGED COHERENCY FUNCTION

Between July 2021 and June 2022, a total of 16 earthquake events were recorded at the target site. Comprehensive descriptions of the array configuration, recording process, signal processing steps, and regression approach can be found in Lee et al. (2024). In this section, only a concise overview of the procedure is provided.

Complex coherency is defined as the ratio of the smoothed cross-spectral density to the geometric mean of the auto power spectra, as expressed below:

$$\gamma_{ij}(\xi_{ij}, \omega) = \frac{S_{ij}(\omega)}{\sqrt{S_{ii}(\omega)S_{jj}(\omega)}} \quad (4)$$

where ξ_{ij} is the separation distance for horizontal direction, $S_{ij}(\omega)$ and S_{ii} or $S_{jj}(\omega)$ are smoothed cross spectrum between stations and smoothed auto power spectra for each station, respectively.

Lagged coherency is one of the most commonly applied measures for assessing ground-motion coherency. It quantifies the similarity between two time-history records after eliminating the temporal offset within a given frequency range. This method is conceptually similar to removing the wave-passage effect from the wavefield; however, it does not assume that the time lag is constant across all frequency bands. In addition, the applied time shift may not match the delay produced by the wave-passage effect of a single plane wave for every station pair (Imtiaz, 2015; Lee et al., 2024). The lagged coherency is obtained by taking the absolute value of the complex coherency (Toksöz et al., 1991), as expressed:

$$\gamma_{ij}^{\text{Lagged}}(\xi_{ij}, \omega) = \left| \frac{S_{ij}(\omega)}{\sqrt{S_{ii}(\omega)S_{jj}(\omega)}} \right| \quad (5)$$

A regression analysis was conducted to formulate an empirical coherency function for the target site, following the framework proposed by Abrahamson & Jeremić (2022). The regression model is expressed in the following form:

$$\begin{aligned} & \tanh^{-1}(\gamma(f, \xi)) \\ &= a_1(\xi) \left[\frac{\pi}{2} - \tan^{-1} \left((f + b_2(\xi)) b_1(\xi) \right) \right] \\ & \quad + a_2(\xi) \exp(-2.5f) \end{aligned} \quad (6)$$

where $a_1(\xi)$, $a_2(\xi)$, $b_1(\xi)$ and $b_2(\xi)$ are site-specific parameters calculated through the regression analysis. f and ξ are frequency and horizontal distance, respectively. Figure 4 shows the empirical lagged coherency for horizontal direction.

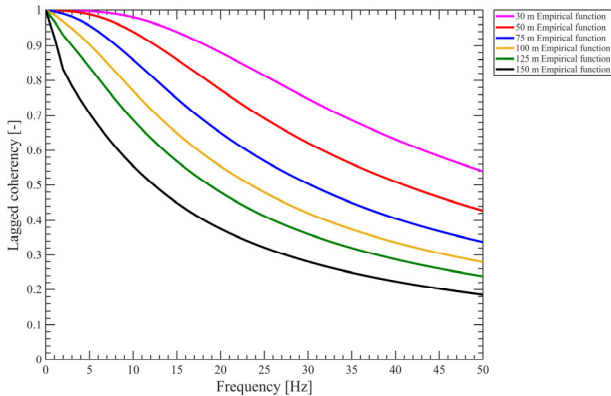


Figure 4. Empirical lagged coherency of target site for horizontal direction.

4 NUMERICAL MODELING

Gaussian model was employed to represent spatial variability at the target site. Random fields were generated in MATLAB R2022a using the reference V_s profile, CV, and CL, following a normal distribution. The spatial correlation was defined by a Gaussian function of separation distance τ , as given in Equation (3).

Chang et al. (2022) indicated that, when applying random fields in time-history analyses, the mean and standard deviation of the amplification ratio tend to stabilize after about 30 realizations. Based on this finding, 30 random fields were generated in this study to maintain statistical reliability in the probabilistic analysis. Figure 5 presents a sample realization of the random field.

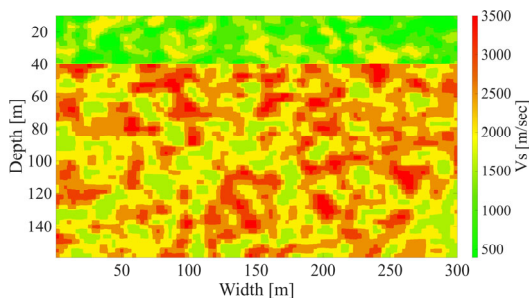


Figure 5. One realization of the generated random fields.

According to Svay et al. (2020), at least 30 seismic records are required to achieve stable coherency analysis. In this study, a total of 30 ground motions were utilized to construct coherency functions, which were organized into three categories. The first category comprised 10 ground motions selected from the PEER database (Ancheta et al., 2014). The second included 10 records obtained from the dense array of target site (Lee et al., 2024). The third consisted of 10 records from the two largest instrumented earthquakes in Korea (Choi

et al., 2019)—the 2016 Gyeongju event (September 12, 2016; Mw 5.4) and the 2017 Pohang event (November 15, 2017; Mw 5.4). All selected motions in these groups had a time step of 0.005 s.

The numerical simulations were carried out using the finite element analysis code OpenSees (Mazzoni et al., 2006). Since the target site consists of hard rock with a V_s exceeding 1,000 m/s, linear material properties were applied in the element modeling. To indirectly simulate free-field conditions, equal degrees of freedom constraints were imposed on the lateral boundaries. To absorb downward-propagating shear waves and to simulate the propagation of input ground motions, horizontal viscous dampers were installed at the bottom boundary of the computational model. To represent energy dissipation under small strain level, full Rayleigh damping formulation was applied. The element height was modeled as 1 m, following the recommendation of Kuhlemeyer & Lysmer (1973), which is less than 1/10 of the minimum wavelength of seismic waves corresponding to the target frequency of 50 Hz in this study.

The range of response extraction nodes for the coherency analysis was set to 150 m, corresponding to the maximum station-to-station distance at the target site. Following the recommendation of Chang et al. (2022), the width of the numerical model was set to twice the range of the extraction nodes. The analysis depth was set to 150 m, consistent with the depth used in the coherency analysis for a rock site by Lee et al. (2025).

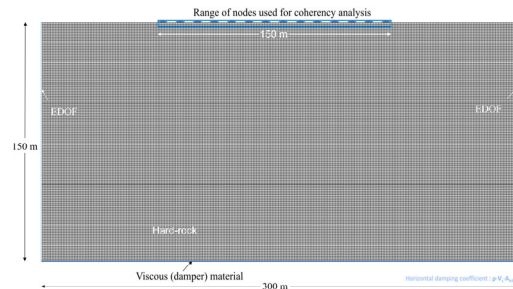


Figure 6. Computational model in OpenSees.

5 NUMERICAL LAGGED COHERENCY FUNCTION

Figure 7 compares the empirical model developed for the target site, as reported by Lee et al. (2024), with the numerically derived model. The agreement between the two functions demonstrates that Gaussian random fields, calibrated using detailed geophysical investigations, effectively represent the local subsurface variability of the target site. These indicate that, when site-specific CV and CL values are available, numerical simulations can successfully reproduce lagged coherency functions that were originally obtained through empirical methods.

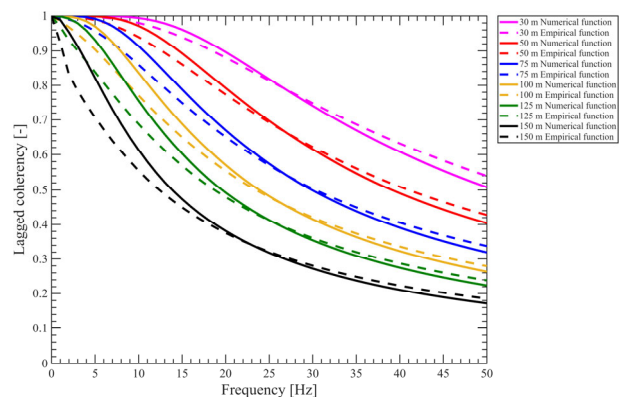


Figure 7. Numerical lagged coherency of target site for horizontal direction.

6 CONCLUSIONS

This study examined the feasibility of developing site-specific coherency functions through numerical simulations informed by spatial variability parameters derived from in-situ investigations. Extensive field tests were conducted at a rock site in Korea, to characterize the subsurface conditions and estimate CV and CL profiles based on V_s data obtained from SPS tests as well as HVSR analyses. The results indicated that CV decreases, and CL increases with depth, suggesting a more homogeneous rock mass at greater depths. These depth-dependent profiles were used to generate Gaussian random fields for the numerical modeling.

Time-history analyses were carried out using the finite element code OpenSees, combining 30 realizations of the random fields with 30 input ground motions, resulting in a total of 900 simulations. The numerically derived lagged coherency functions for horizontal direction were compared with the empirical lagged coherency function obtained from a dense array at the target site. The comparison showed strong agreement, demonstrating that physics-based simulations, when calibrated with detailed site characterization, can successfully reproduce observed spatial variability. This workflow highlights the potential of integrating V_s profiles and spatial variability parameters into numerical analyses as a practical alternative to the time- and resource-intensive deployment of dense arrays for empirical data collection.

Nevertheless, several essential tasks remain for future work:

1. Conducting sensitivity analyses of the computational model (e.g., number of analyses, width, depth, and element size) to ensure appropriate conditions for coherency analysis.
2. Performing additional validation of numerical lagged coherency function for vertical direction.
3. Developing and validating numerical plane-wave coherency functions in both horizontal and vertical directions for application to incoherency SSI analyses.

Addressing these points in future research will be essential to further refine and expand the applicability of the proposed methodology.

7 ACKNOWLEDGEMENTS

This research was supported by Korea Hydro & Nuclear Power Co. Ltd. and National Research Foundation of Korea (NRF) grant funded by the Korea government (MSIT) [NRF-2022R1A2C3003245].

8 REFERENCES

Abrahamson, N.A. & Jeremić, B., 2022. Generation of spatial coherency models suitable for Korean NPP sites. Technical consulting report prepared for KEPCO E&C Co., Inc.

Abrahamson, N.A., 2007. Hard-rock coherency functions based on the Pinyon Flat Array data. Piedmont: Electric Power Research Institute (EPRI).

Ancheta, T.D., Stewart, J.P. & Abrahamson, N.A., 2011. Engineering characterization of earthquake ground motion coherency and amplitude variability.

Ancheta, T.D., Darragh, R.B., Stewart, J.P., Seyhan, E., Silva, W.J., Chiou, B.S.-J., Wooddell, K.E., Graves, R.W., Kottke, A.R. & Boore, D.M., 2014. NGA-West2 database. *Earthquake Spectra*, 30(3), pp.989–1005.

Baecher, G.B. & Christian, J.T., 2003. Discussion of “Evaluating site investigation quality using GIS and geostatistics” by RL Parsons

and JD Frost. *Journal of Geotechnical and Geoenvironmental Engineering*, 129(9), pp.867–867.

Choi, I., Ahn, J.-K. & Kwak, D., 2019. A fundamental study on the database of response history for historical earthquake records on the Korean Peninsula. *KSCE Journal of Civil and Environmental Engineering Research*, 39(6), pp.821–831.

El Haber, E., Cornou, C., Jongmans, D., Lopez-Caballero, F., Abdelmassih, D.Y. & Al-Bittar, T., 2021. Impact of spatial variability of shear wave velocity on the lagged coherency of synthetic surface ground motions. *Soil Dynamics and Earthquake Engineering*, 145, 106689.

Imtiaz, A., 2015. *Seismic wave field, spatial variability and coherency of ground motion over short distances: near source and alluvial valley effects*. Université Grenoble Alpes.

Ghiocel, D.M., Jang, Y., and Lee, I., 2017. Understanding seismic motion incoherency modeling and effects on SSI and SSSI responses of nuclear structures. *Proceedings of the 24th Conference on Structural Mechanics in Reactor Technology*.

Kuhlemeyer, R.L. & Lysmer, J., 1973. Finite element method accuracy for wave propagation problems. *Journal of the Soil Mechanics and Foundations Division*, 99(5), pp.421–427.

Lee, D. et al., 2025. Sensitivity analysis of numerical coherency model for rock sites. *Applied Sciences*, 15(6).

Lee, Y., Lee, D., Kim, H.-S., Park, J.-S., Jung, D.-Y., Kim, J., Kim, D.Y., Lee, Y. & Park, D., 2024. Spatial coherency analysis of seismic motions from a hard rock site dense array in Busan, Korea. *Bulletin of Earthquake Engineering*.

Luco, J. & Wong, H., 1986. Response of a rigid foundation to a spatially random ground motion. *Earthquake Engineering & Structural Dynamics*, 14(6), pp.891–908.

Mazzoni, S., McKenna, F., Scott, M.H. & Fenves, G.L., 2006. OpenSees command language manual. *Pacific Earthquake Engineering Research (PEER) Center*, 264(1), pp.137–158.

Rathje, E.M., Kottke, A.R. & Trent, W.L., 2010. Influence of input motion and site property variabilities on seismic site response analysis. *Journal of Geotechnical and Geoenvironmental Engineering*, 136(4), pp.607–619.

Svay, A., Perron, V., Imtiaz, A., Zentner, I., Cottreau, R., Clouteau, D., Bard, P.Y., Hollender, F. & Lopez-Caballero, F., 2017. Spatial coherency analysis of seismic ground motions from a rock site dense array implemented during the Kefalonia 2014 aftershock sequence. *Earthquake Engineering & Structural Dynamics*, 46(12), pp.1895–1917.

Toksöz, M.N., Dainty, A.M. & Charrette, E.E., 1991. Coherency of ground motion at regional distances and scattering. *Physics of the Earth and Planetary Interiors*, 67(1–2), pp.162–179.